Materials Research. 2018; 21(suppl. 2): e20170875
DOI: http://dx.doi.org/10.1590/1980-5373-MR-2017-0875

Annealing and Extended Etching Improve a Torsional Resonator for Thin Film Internal Friction Measurements

***Thomas Metcalf*[a]*, *Xiao Liu*[a], *Matthew Robert Abernathy*[b]**

[a]*U.S. Naval Research Laboratory, Code 7130, Washington, District of Columbia, 20375, United States of America*
[b]*NRC Postdoctoral Associate, U.S. Naval Research Laboratory, Washington, District of Columbia 20375, United States of America*

Received: September 27, 2017; Revised: March 01, 2018; Accepted: April 20, 2018

We evaluate two methods to improve the background internal friction of the Double Paddle Oscillator (DPO), which has a nominal low temperature value of $Q^{-1} \approx 2\times10^{-8}$. We find that annealing the DPO in vacuum at 300°C for 3 hours systematically reduced Q^{-1} at all temperatures and revealed a 100K internal friction peak by permanently removing it. We also find a striking decrease of low temperature Q^{-1} as the DPO geometry is altered through extended etching. This decrease is evaluated via Finite Element Method modeling in terms of mode mixing and attachment loss.

Keywords: *Thin film internal friction, silicon internal friction.*

1. Introduction

For more than 40 years, the internal frictions of thin film materials have been measured by depositing the films onto resonators with high quality factors and measuring the change of both resonant frequency and quality factor of the resonator.[1] This measurement requires a resonator substrate with a sufficiently low background mechanical loss such that the total mechanical loss of a film-laden resonator is measurably greater than that of the bare resonator. The additional mechanical damping provided by a thin film deposited onto a resonator is given by the internal friction of the film scaled by the ratios of the film and substrate thicknesses and elastic moduli. As such, it is desirable to lower the mechanical loss of the bare resonator, which allows more sensitive measurements, of thinner, softer, or less lossy films.

One resonator which provides an excellent platform for thin film internal friction measurements is the double paddle oscillator, or DPO.[2,3] It is pictured in the inset to Figure 1. It is approximately 29mm tall. From the top, its sections are referred to as the head, neck, wings, leg, and foot. In a typical measurement, the bottom of the foot (below the line) is held in a clamp while the wings are excited and detected electrostatically via metal film electrodes deposited onto the wings. The 8th mechanical resonance (in ascending order of frequency) of this resonator is referred to as the 2nd anti-symmetric mode, or AS2. It is an audiofrequency mode with a resonant frequency between 5 kHz and 7 kHz. The out-of-plane motion of this mode is illustrated in the color scale and wireframe of the inset to Figure 1. The head and wings vibrate out of phase with one another, twisting the neck. The motion of the head and wings balance each other and as a result there is very little twisting of the leg. The metal film electrodes, which travel down the leg, do not cover the areas of high strain on the wings. A film deposited onto the neck is measured largely in shear deformation. A companion resonator, termed the Young's Modulus Resonator (YMR), uses a similar scheme for flexural deformations,[4] and the annealing results discussed below should apply to the YMR as well.

At low temperatures, the AS2 mode of the DPO has an extremely high quality factor. (The high temperature quality factor is dominated by thermoelastic loss).[5] Figure 1 shows three characterizations of the quality factor: the original bare DPO measurements, published by White and Pohl in 1995;[6] a curve representing a typical bare resonator Q^{-1}; and a data set from a recent DPO. It is evident that the Q^{-1} of bare DPOs has improved since their introduction, allowing more sensitive measurement of thin films. In this paper, we discuss two systematic and repeatable effects which contribute to these improved quality factors.

2. Fabrication and Measurement

Because the details of fabrication play a significant role in the observed improvement of the quality factor, we will describe them in detail. The DPO is fabricated from single-crystal, float-zone, high-purity, double-side polished, [100] oriented silicon wafers, traditionally 0.3mm thick, although other thicknesses have been used.[7] Before fabrication, the wafers are put through the RCA cleaning process, after which they are coated with silicon nitride using low-pressure chemical vapor deposition (LPCVD).

*e-mail: tom.metcalf@nrl.navy.mil

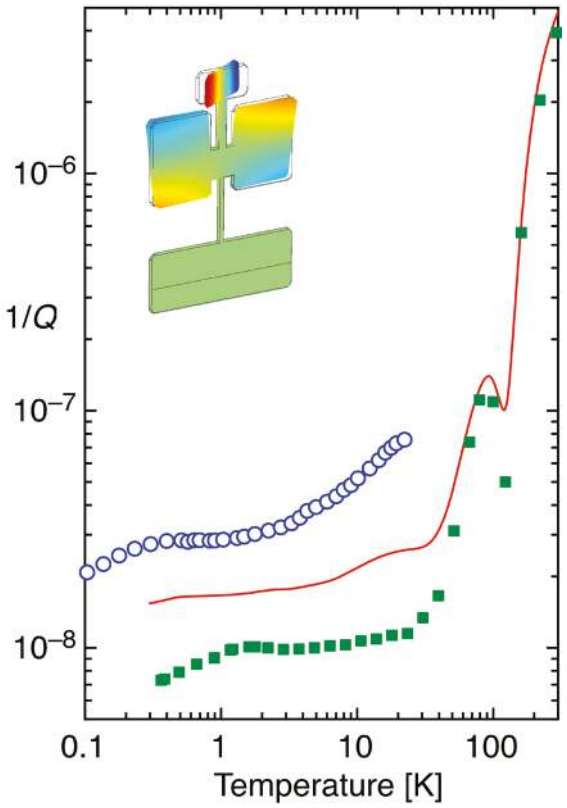

Figure 1. Inverse Quality Factor (Q^{-1}) versus Temperature for original DPO (blue open circles), our standard DPO (red solid curve), and a recent DPO (green solid squares). Inset: illustration of DPO resonator. Color scale indicates out-of-plane displacement at AS2 oscillation maximum; wireframe shows equilibrium position.

The DPO pattern is transferred using standard photolithography. After photoresist (typically Shipley 1813) is spun and baked onto a wafer, the wafer is cleaved in half along a <110> axis in order to align the edges of the DPO geometry on the photolithographic mask precisely to the crystallographic axes of the wafer. The photoresist is exposed and developed, after which the silicon nitride is etched in a reactive ion etching (RIE) process. This etching consists of 30 sccm of tetrafluoromethane at 10 mTorr, with 50W of plasma power for 5 minutes. The RIE step results in DPO shapes of silicon nitride atop bare silicon. The silicon nitride then acts as a mask for the release step, in which the silicon surrounding the DPO is etched in a concentrated (20% by weight) potassium hydroxide (KOH) solution held at 85°C for 4-6 hours. The etch rate for {100} faces (i.e. the top of the wafer) is 1-2 orders of magnitude faster than for {111} faces,[8,9] resulting a DPO with beveled {111} edges and a bottom face which extends approximately 212μm beyond the top face along all edges.

Before use, the silicon nitride layer is removed by etching in 25% hydrofluoric acid for 15 minutes, after which metal film electrodes are deposited on the bottom of the wings, leg, and foot. The electrodes consist of a 5nm adhesion layer followed by a 50nm metal layer and are either chromium followed by gold, or titanium followed by platinum. These electrodes remained throughout all further processing steps.

3. Annealing

The background damping of a bare DPO is reduced upon moderate annealing, revealing two energy loss mechanisms that are present in the as-released DPO. Shown in Figure 2(a) are Q^{-1} versus temperature measurements for an otherwise bare DPO before and after annealing for 3 hours at 300°C in a tube furnace under high vacuum.

This is a comparatively gentle annealing: during the preparation of the silicon wafers, they are heated to 800°C as a part of the LPCVD silicon nitride coating step. Since any defects which anneal out at 300°C should also anneal out at 800°C, we conclude that the loss mechanisms are likely introduced during the DPO fabrication procedure.

Figure 2(b) shows the change in quality factor, $\Delta Q^{-1} = Q^{-1}_{\text{measured}} - Q^{-1}_{\text{annealed}}$, after several treatment steps. These values represent energy loss mechanisms that are removed upon annealing or which arise during treatment.* The ΔQ^{-1} of the as-released DPO, although small, increases with increasing temperature, from approximately 3×10^{-9} at the lowest measurements, to 2×10^{-8} near 100K. Above 100K, the overall Q^{-1} of the resonator becomes too high (because of thermoelastic damping[5]) in order to resolve such small changes. Overall the appearance is of a broad internal friction peak centered near 100K.

After annealing, the DPO was allowed to age for 4 months while kept in a wafer tray and exposed to ordinary laboratory air, after which two measurements of the annealed-and-aged DPO were made. The subsequent ΔQ^{-1} values are shown in Figure 2(b) as well. At the lowest temperatures, the ΔQ^{-1} is the same as for the as-released indicating that the Q^{-1} has reverted to the pre- annealing value. The high-temperature peak, however, has not returned. Thus we infer that there are two energy loss mechanisms present in the as-released DPO which are removed upon annealing: one which contributes a uniform loss of $\Delta Q^{-1} \approx 3 \times 10^{-9}$ over the entire temperature range, and which returns upon aging; and the broad 100K peak which is permanently removed during annealing.

To further investigate the nature of the peak, the DPO was subjected to a second RIE treatment. The RIE processing, although used to etch silicon nitride, also etches silicon. Without the benefit of the silicon nitride layer, this step introduces surface damage across the DPO and an associated broad-based mechanical loss. The ΔQ^{-1} values post-RIE, also shown in Figure 2(b), show a new background value, $\Delta Q^{-1} \approx 8 \times 10^{-9}$, across all temperatures, and additionally shows a rise at $T > 30$K, coinciding with the as-released values. After the RIE step, the DPO was annealed a second time, and the post-anneal-after-RIE measurements are shown as well. This annealing step was unable to repair the

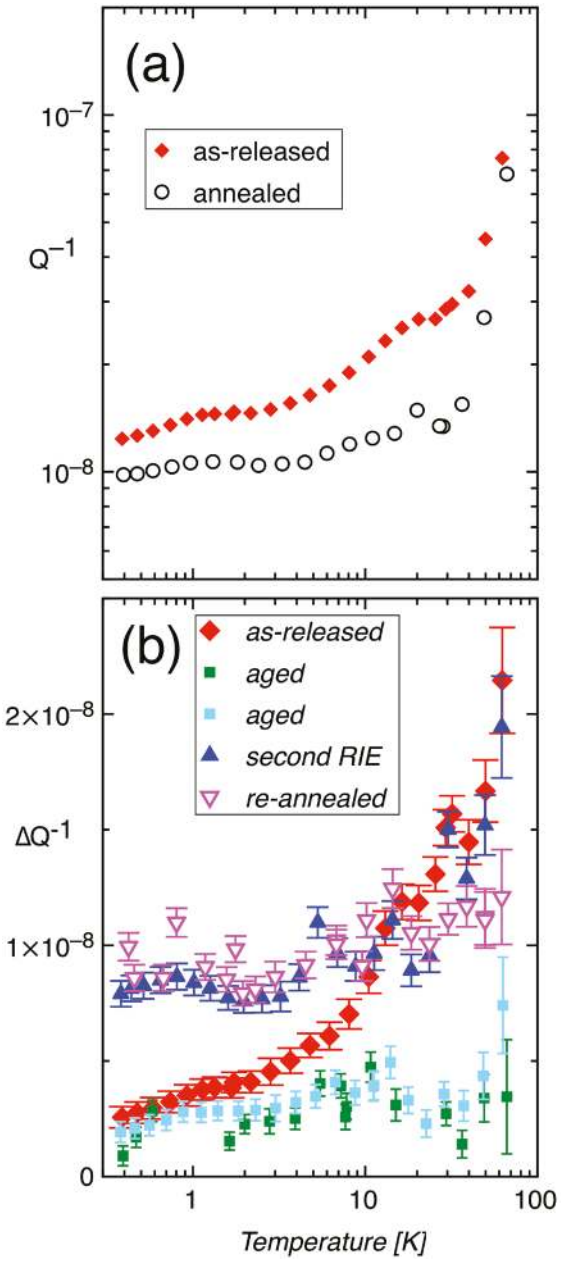

Figure 2. (a) Inverse Quality Factor (Q^{-1}) of an as-released DPO (red closed diamonds) and the same DPO after an annealing step (black open circles), as a function of temperature. **(b)** Change in Inverse Quality Factor, (Q^{-1}, between annealed DPO (black open circles of (a)) and DPO as released (red solid diamonds), after 4 months aging (green, blue solid squares), following an RIE treatment (blue solid upwards triangles), and after a second annealing after RIE (pink open down triangles). Note logarithmic y-axis in (a); linear y-axis in (b).

broad-based damage that increased the background damping of this DPO. However, the measurements above 30K show ΔQ^{-1} values consistent with the new background level and lower than the as-released and RIE values. It appears as if the RIE treatment re-introduced the 100K peak, and the subsequent annealing removed it.

4. Etching Geometry

The final shape of the DPO depends upon the amount of time it is left in the KOH etch bath during the release step of fabrication. The minimal etch time is that required to etch through the entire thickness of the silicon wafer. The top and bottom faces of the DPO consist of {100} faces, protected from the KOH by silicon nitride. The edges consist of {111} faces, which are an intrinsic etch stop in the KOH etching process. The shape of the exterior corners is more complicated, but Shikida, et al., have identified the faces that emerge during etching: two {311} faces and two smaller {110} faces, as shown in Figure 3(a).[10] These etch rapidly. If the DPO is held in the etch bath after it has been released, the corners will continue to etch while the {111} edges remain mostly fixed. This results in an appearance which looks increasingly rounded as the etching progresses, as illustrated in Figures 3(b) and (c). The greater the degree of etching, the higher the frequency, as the moment of inertia (particularly of the DPO head) decreases.

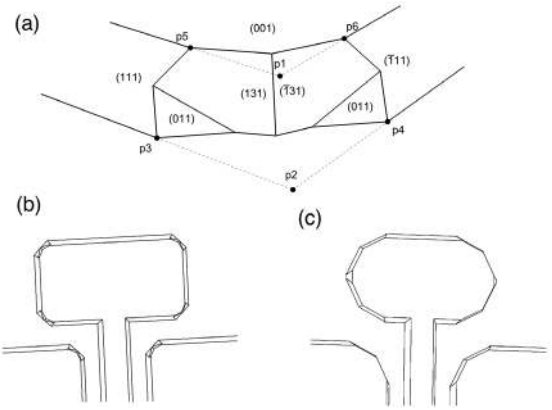

Figure 3. (a) Illustration of exterior corner of a DPO, with crystallographic faces and some of the points used in the construction labeled. **(b)** Close-up of head of a DPO with corners etched to Etch Parameter 1.5. **(c)** Close-up of head of DPO with corners etched to Etch Parameter 4.5.

The increased etching appears to improve the quality factor. Figure 4 shows Q^{-1} measured at low temperature (near 400mK) as a function of resonator frequency, for several DPO resonators. For frequencies below 6 kHz, there appears to be a noisy but sharp drop of Q^{-1} with increasing frequency. Above 6 kHz, the Q^{-1} appears to level off, but at a significantly lower value than at lower frequencies.

To understand why the increase of frequency might decrease Q^{-1}, we examine a Finite-Element-Method (FEM) model of the DPO. The model is illustrated in Figure 3(a). The etch begins with a square corner shown by the dashed lines and the {311} faces grow as the etch progresses. The degree of etching is modeled by choosing the distance between p1 and p5, a distance labeled as the "etch parameter". The

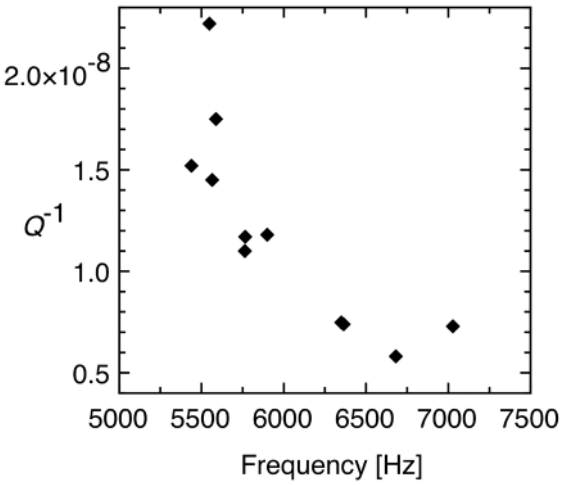

Figure 4. Low-temperature (400 mK) Q^{-1} versus low-temperature frequency for several DPO resonators.

distance between p2 and p3 is then calculated based on relative etch rates of the different crystallographic planes. With these distances determined, the points, edge, and faces that comprise the corner are determined with analytic geometry. An etch parameter value of 1.5 gives corners as shown in Figure 3(b) and corresponds to removing a DPO from the KOH etch bath as soon as the DPO is fully released, and an etch parameter value of 4.5 gives the more rounded corners shown in Figure 3(c), which corresponds to leaving the released DPO in the KOH etch bath for additional time (1-2 hours) after release. Further etching cannot be modeled in this scheme because the {311} facets of adjacent corners would overlap and the calculations would no longer represent the physical facets.

Figure 5(a) shows that FEM calculations of the AS2 mode frequency increase with increasing etch parameter, as expected. Also shown in Figure 5(a) are calculated frequencies of the 7th resonance mode, known as the Flapping Mode (FL). The deformation in FL is almost entirely flexural, with the head and both wings bending in the same direction. It has a much lower Q than AS2.[2] The modal spacing between FL and AS2 increases with increased etching. The further apart the frequencies of the modes, the less mixing there will be between then, and the less energy of a rung-up AS2 mode would bleed into the FL mode.

The FEM models can also calculate the ratio of strain energy in the foot of the DPO to the total strain energy in the entire DPO. Presumably, the lower this ratio, the lower the energy loss at the attachment will be. This method of estimating clamping losses has been used to compare modes of the DPO[2] and to design the YMR.[11] Figure 5(b) shows this ratio as a function of etch parameter. The ratio decreases nearly linearly with increasing etch parameter, indicating that clamping loss is reduced with increased etching.

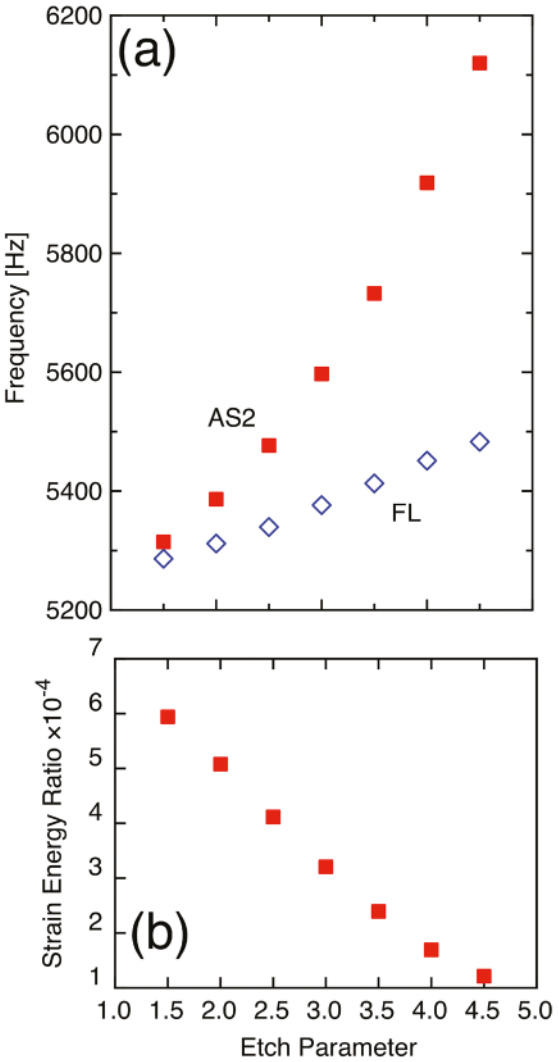

Figure 5. (a) Frequency of AS2 (red solid squares) and FL (blue open diamonds) modes as a function of Etch Parameter, for FEM modeled DPOs. **(b)** Ratio of strain energy in foot to total strain energy in DPO, as a function of Etch Parameter. Note 10^{-4} scaling of ratio.

Whether the improvement in Q^{-1} with increasing frequency below 6 kHz is the result of reduced modal mixing or lower strain energy in the foot, it appears there is another energy loss mechanism with $Q^{-1} \approx 7 \times 10^{-9}$ that dominates the DPO Q^{-1} above 6 kHz.

5. Conclusions

To create resonators with the highest possible quality factors, as many energy loss mechanisms as possible must be eliminated. We have shown that standard microfabrication techniques likely introduce unexpected loss mechanisms in silicon resonators. Fortunately, a relatively gentle annealing step appears to eliminate them. We have also shown that apparently minor differences in resonator geometry can

have a large influence on final resonator Q^{-1}. A systematic and parametric FEM modeling of candidate resonator designs can be used to minimize both mode mixing and attachment losses.

6. Acknowledgements

This work funded by the Office of Naval Research.

7. References

1. Berry BS, Pritchet WC. Vibrating Reed Internal Friction Apparatus for Films and Foils. *IBM Journal of Research and Development*. 1975;19(4):334-343.

2. Liu X, Morse SF, Vignola JF, Photiadis DM, Sarkissian A, Marcus MH, et al. On the modes and loss mechanisms of a high *Q* mechanical oscillator. *Applied Physics Letters*. 2001;78(10):1346-1348.

3. Spiel CL, Pohl RO. Normal modes of a Si(100) double-paddle oscillator. *Review of Scientific Instruments*. 2001;72(2):1482-1491.

4. Metcalf TH, Liu X. An ultra-high *Q* silicon compound cantilever resonator for Young's modulus measurements. *Review of Scientific Instruments*. 2013;84(7):075001.

5. Photiadis DM, Houston BH, Liu X, Bucaro JA, Marcus MH. Thermoelastic loss observed in a high Q mechanical oscillator. *Physica B: Condensed Matter*. 2002;316-317:408-410.

6. White BE Jr, Pohl RO. Internal Friction of Subnanometer *a*-SiO_2 Films. *Physical Review Letters*. 1995;75(24):4437-4439.

7. Shakeel H, Metcalf TH, Pomeroy JM. Analysis of Thickness and Quality factor of a Double Paddle Oscillator at Room Temperature. In: *Proceedings of the 2016 IEEE Sensors Conference*; 2016 Oct 30-Nov 3; Orlando, FL, USA. DOI: 10.1109/ICSENS.2016.7808783

8. Sato K, Shikida M, Matsushima Y, Yamashiro T, Asaumi K, Iriye Y, et al. Characterization of orientation-dependent etching properties of single-crystal silicon: effects of KOH concentration. *Sensors and Actuators A*. 1998;64(1):87-93.

9. Seidel H, Csepregi L, Heuberger A, Baumgärtel H. Anisotropic Etching of Crystalline Silicon in Alkaline Solutions. I. Orientation Dependence and Behavior of Passivation Layers. *Journal of the Electrochemical Society*. 1990;137(11):3612-3626.

10. Shikida M, Nabara K, Koizumi T, Sasaki H, Odagaki M, Sato K, et al. A model explaining mask-corner undercut phenomena in anisotropic silicon etching: a saddle point in the etching-rate diagram. *Sensors and Actuators A: Physical*. 2002;97-98:758-763.

11. Metcalf TH, Liu X. An Ultra-High Q Silicon Cantilever Resonator for Thin Film Internal Friction and Young's Modulus Measurements. *Solid State Phenomena*. 2012;184:325-330.

* Each measurement has an intrinsic error of 2.5%, and a temperature-dependent error determined by equilibration times and the temperature sensitivity of Q^{-1}. These errors then determine the error of the spline fits to Q^{-1}_{annealed} versus T. The spline fit errors are combined in quadrature with the Q^{-1}_{measured} error to determine the error bars.